

## Application of Fenton and photo-Fenton process for decolorization of Direct Red 80 dye from synthetic wastewater

Masoumeh Sheikh Hosseini Lori<sup>a,b</sup>, Mohammad Mehdi Amin<sup>b,c</sup>, Mohammad Kamranifar<sup>d</sup>, Ali Fatehizadeh<sup>b,c</sup>, Mohammad Reza Zare<sup>e</sup>, Mohammad Ghasemian<sup>b,c</sup>, Ensiyeh Taheri<sup>b,c,\*</sup>

<sup>a</sup>Student Research Committee, School of Health, Isfahan University of Medical Sciences, Isfahan, Iran, email: masoomeh\_shhosseini72@yahoo.com (M.S.H. Lori)

<sup>b</sup>Department of Environmental Health Engineering, School of Health, Isfahan University of Medical Sciences, Isfahan, Iran, Tel. +98 313 792 3296; Fax: +98 313 669 5849; emails: e\_taheri\_83@yahoo.com (E. Taheri), amin@hlth.mui.ac.ir (M.M. Amin), fatehizadeh@gmail.com/a.fatehizadeh@hlth.mui.ac.ir (A. Fatehizadeh), ghasemian2005@gmail.com (M. Ghasemian)

<sup>c</sup>Environment Research Center, Research Institute for Primordial Prevention of Non-Communicable Disease, Isfahan University of Medical Sciences, Isfahan, Iran

<sup>d</sup>Department of Environmental Health Engineering, Faculty of Health, Social Determinants of Health Research Center, Birjand University of Medical Sciences (BUMS), Birjand, Iran, email: mo.kamrani@yahoo.com (M. Kamranifar)

<sup>e</sup>Department of Environmental Health Engineering, School of Health, Larestan University of Medical Sciences, Larestan, Iran, email: zaremohammad1363@yahoo.com (M.R. Zare)

Received 8 February 2020; Accepted 13 June 2020

---

### ABSTRACT

The present study was performed to evaluate the efficiency of Fenton (FP) and photo-Fenton (PFP) processes for direct red 80 (DR80) dye removal from synthetic wastewater. The effects of primary variables viz solution pH, contact time, Fe<sup>2+</sup> concentration, H<sub>2</sub>O<sub>2</sub> dose, and DR80 concentration on DR80 removal by FP and PFP were examined. The results showed that DR80 removal in acidic pH is higher than that of alkaline pH. Moreover, in both processes, with increasing the contact time, Fe<sup>2+</sup> concentration, and H<sub>2</sub>O<sub>2</sub> dose, the DR80 removal efficiency improved. However, with increasing initial DR80 concentration, the removal efficiency decreases. Under optimum conditions for FP (solution pH: 2, H<sub>2</sub>O<sub>2</sub> dose: 80 mg/L, contact time: 35 min, Fe<sup>2+</sup> concentration: 35 mg/L, and initial DR80 concentration: 20 mg/L), the highest DR80 removal efficiency was obtained (95%). Also, at initial DR80 concentration of 20 mg/L and optimal conditions for PFP (solution pH: 2, contact time: 20 min, H<sub>2</sub>O<sub>2</sub> dose: 15 mg/L, and Fe<sup>2+</sup> concentration: 2 mg/L), the DR80 removal efficiency reached to 99.5%. The results demonstrating that the PFP has higher ability for DR80 removal in a short time than FP using significantly lower amount of H<sub>2</sub>O<sub>2</sub> and Fe<sup>2+</sup>. The empirical model yielded a R<sup>2</sup> of 0.81 and 0.72 for FP and PFP, respectively, and indicating relatively good describe of DR80 removal efficiency under different conditions. The sensitivity analysis showed that the solution pH implying the strongest effect on DR80 removal efficiency for both FP and PFP. The significant difference between costs of FP and PFP was achieved and is due to the electrical energy of mixing for high contact time in FP process.

*Keywords:* Cost evaluation; Direct Red 80; Fenton; Photo-Fenton; Sensitivity analysis

---

\* Corresponding author.

## 1. Introduction

The dyes are classified as an important raw materials used in industries including textiles, leather, cosmetics, paper, printing, plastics, pharmacy, and food processing [1]. At the current time, around the world, about 700,000 tons dyes including 10,000 types of pigments are produced annually and a significant part of these products releases to the environment via wastewater from various industries [2]. For example, about 15% of the total dyes consumed in the dyeing processes industries discharges into the wastewaters [3]. In this regard, the textile wastewater is a major problem for conventional wastewater treatment [4]. The effluent of textile industries contains various compounds, including chemicals, suspended solids, toxic compounds, and dyes [5]. Based on chemical structure of dyes, they are classified into azo, anthraquinone, xanthine, acridine, flavin, and so on [6]. The direct red 80 (DR80) is belong to azo dyes categories which is the largest dye categories consumed in industry [7]. The chemical structure of DR80 are shown in Fig. 1. This group of dyes has one or more azo bonds (–N=N–) and aromatic rings, making it toxic, and mutant for living organisms [8].

In addition, the various studies have shown that the dyes used in the textile industry have carcinogenic properties and also cause allergies, dermatitis, and skin irritation [6]. Therefore, the discharging of these kinds of wastewaters into the environment without adequate treatment causes many problems for the life of aquatic animals and human health [4]. The conventional methods for removing dye from textile industry include coagulation/ flocculation and adsorption by active carbon. However, both mentioned methods producing high amount of sludge and waste, which need more treatment for their disposal [9]. The biological treatment of wastewater and water pollutants is often cheaper than other treatment options. However, textile dyes are resistant to biodegradation and this method is not appropriate for the treatment of colored wastewaters [10]. In recent years, innovative technologies such as advanced oxidation processes (AOPs) have been used to degrade various organic pollutants [11].

The various types of AOPs are including ozonation [12], photocatalytic degradation [13], Fenton processes (FP), and photo-Fenton processes (PFP) [4]. These processes rely on the production of free radicals, the most important of them is radical hydroxyl ( $\cdot\text{OH}$ ) [14].

Among these processes, FP and PFP can be considered as an efficient way to degrade various types of refractory organic compounds. These processes are able to oxidize organic compounds and transform them into non-harmful substances, mineralize them, and produce end products such

as  $\text{CO}_2$  and  $\text{H}_2\text{O}$  [15]. The FP involves the reaction between dissolved  $\text{Fe}^{2+}$  and  $\text{H}_2\text{O}_2$  in aqueous acidic solution, which leads to the oxidation of  $\text{Fe}^{2+}$  to  $\text{Fe}^{3+}$  and the production of  $\cdot\text{OH}$  radicals. The main reaction for  $\cdot\text{OH}$  radicals production is based on Eq. (1), after complete conversion of  $\text{Fe}^{2+}$  to  $\text{Fe}^{3+}$ , the reaction is continue automatically [16].



When FP occurred in the presence of the illumination ( $\text{Fe}^{2+}/\text{H}_2\text{O}_2/\text{light}$ ), the rate of pollutants degradation increased due to backing  $\text{Fe}^{3+}$  to  $\text{Fe}^{2+}$  and  $\cdot\text{OH}$  radical production. The process was known as PFP that is like the FP. In addition, irradiation of UV or visible light enhance the production of  $\cdot\text{OH}$  radical and conversion of  $\text{Fe}^{3+}$  to  $\text{Fe}^{2+}$  according to Eq. (2) [16].



The different studies used FP and PFP for degradation of various pollutants. Tarkwa et al. [17] studied decomposition of orange G dye by PFP and reported that 93% removal of total organic carbon was achieved under optimal condition. Sohrabi et al. [18] investigated carmoisine edible dye removal and found that the PFP is able to obtained 95% removal efficiency [18]. Also, the results of Mousavi et al. [19] study showed that FP is able to remove 58% of Rodamin B dye.

In this study, the FP and PFP as a high-performance AOPs was investigated for DR80 removal from synthetic wastewater. The present study was conducted to examine the effects of various variables viz solution pH, contact time,  $\text{Fe}^{2+}$  concentration,  $\text{H}_2\text{O}_2$  dose, and initial DR80 concentration. Furthermore, the proposed empirical model was developed and applied for the quantitative removal of DR80 using the FP and PFP and in order to determine effect of studied variables on the DR80 removal rate, the Monte Carlo simulator was used. To the best of our knowledge, the cost evaluation of FP and PFP for DR80 removal and ordering the fraction of empirical model via sensitivity analysis, that was done in this study, make an interesting approach for comparison between both process for DR80 removal.

## 2. Materials and methods

### 2.1. Chemicals and instrument

In this study, DR80 dye ( $\text{C}_{45}\text{H}_{26}\text{N}_{10}\text{Na}_6\text{O}_{21}\text{S}_6$ ) was obtained from Baharjin Textile Factory (Iran). The other chemicals including  $\text{H}_2\text{O}_2$  (35%),  $\text{FeSO}_4 \cdot 7\text{H}_2\text{O}$ ,  $\text{NaOH}$ , and  $\text{HCl}$

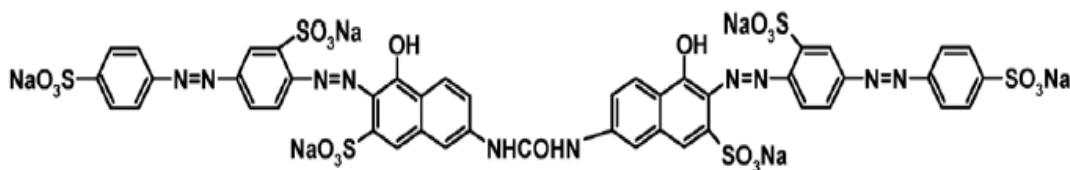


Fig. 1. Chemical structure of DR80 [7].

were analytical grade and purchased from the Merck Co., (Germany). The working solutions were prepared with deionized water. In order to solution pH adjustment, the precalibrated glass body (CG 824 SCHOTT) and NaOH and HCl (0.1 M) were used. The DR80 concentration was measured using by the UV-vis spectrophotometer at  $\lambda_{\max}$ : 525 nm (DR5000 spectrophotometer, HACH, Germany).

## 2.2. FP and PFP experiments

The FP and PFP experiments were carried out in lab scale with a plexiglass reactor (total volume: 1.5 L and working volume: 1 L) and reactor was equipped with UV lamp (150 W with predominantly emitting at of 254 nm) as the radiation source. The UV lamp were immersed in the solution and coated with quartz tubes. It should be noted that for protect against UV radiation, the reactor was covered with aluminum foil. In order to maintain a solution temperature at  $20^{\circ}\text{C} \pm 3^{\circ}\text{C}$ , reactor was equipped with a cooling water bath. During the reactions, the solution pH was uncontrolled. The experiments were initiated with pouring prespecified concentration of DR80 in reactor. Then, effective parameters on DR80 removal by FP and PFP includes solution pH, contact time, Fe,  $\text{H}_2\text{O}_2$ , and DR80 concentration were investigated as summarized in Table 1.

During experiments, a magnetic stirrer at a stable rate (125 rpm) was used to perfect mixing.

## 2.3. Analysis

Upon completion of the contact time, the suspension was filtered through 0.45  $\mu\text{m}$  paper filter (Whatman, No. 42) and analyzed for DR80 concentration. In order to calculate FP and PFP removal efficiency, Eq. (3) was used.

$$R(\%) = \frac{C_0 - C_e}{C_0} \times 100 \quad (3)$$

where  $R$  is DR80 removal efficiency (%),  $C_0$  and  $C_e$  are, respectively, influent and effluent DR80 concentration.

## 3. Results and discussion

### 3.1. Effect of solution pH

In order to evaluate the effect of solution pH, the DR80 removal was studied by FP and PFP under various solution pH. As shown in Fig. 2, in both processes, the DR80 removal efficiency was decreased with solution pH increment, and the highest efficiency was found at acidic pH. In case of FP, the highest DR80 removal efficiency was 79% and obtained at solution pH of 2. In addition, PFP showed that the DR80 removal efficiency decreased from 99.5% to 67.4% with increasing of solution pH from 2 to 9.

It may be inferred that solution pH variation significantly affects the DR80 removal and the removal efficiency is higher in acidic pH than alkaline pH. The strong dependence of FP and PFP efficiency on solution pH value is due to the stability and generation of different amount of  $\cdot\text{OH}$  radicals. Furthermore, the precipitation of iron as hydroxide and reduction of oxidation potential of  $\cdot\text{OH}$  radicals leads to

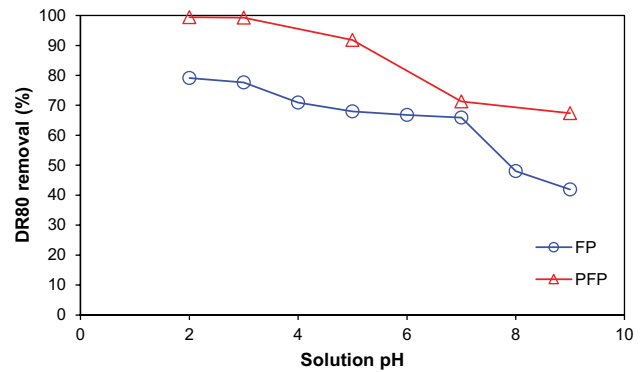
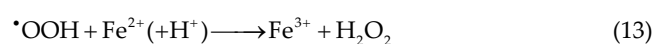
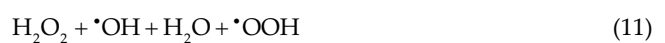
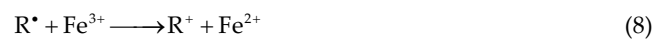
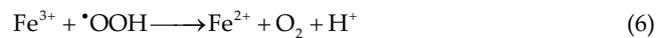
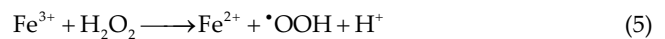
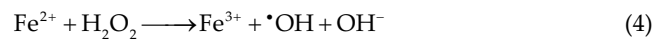


Fig. 2. Variation of DR80 removal efficiency as a function of solution pH by FP and PFP (initial DR80 concentration: 40 mg/L, contact time: 60 min,  $\text{Fe}^{2+}$  concentration: 20 mg/L, and  $\text{H}_2\text{O}_2$  dose: 20 mg/L).

decrease the removal efficiency with increasing pH [18]. In addition, it was established that the oxidation potential of  $\cdot\text{OH}$  radical decreases with increasing pH and that  $\text{H}_2\text{O}_2$  would remain stable at a pH below 2, possibly solving a proton to form an axonium ion ( $\text{H}_3\text{O}^+$ ). The  $\text{H}_3\text{O}^+$  ion allows electrophilic  $\text{H}_2\text{O}_2$  to improve its stability and possibly to significantly reduce ferrous ion reactivity. Then, the amount of  $\cdot\text{OH}$  radicals is reduced and as a result, the removal efficiency of contaminant is reduced [20]. Sohrabi et al. [18] reported that the optimum solution pH for Carmoisine dye removal using FP and PFP was 3.5 [18] that is in agreement with present study. Additionally, Muruganandham et al. [21] demonstrated during dye removal by PFP, the highest dye removal efficiency was obtained at solution pH of 3 [21]. The main reactions performed in the FP and PFP processes are shown in Eqs. (4)–(13).



In PFP, with light irradiation,  $\text{Fe}^{3+}$  is continuously reduced to  $\text{Fe}^{2+}$  according to Eq. (14).



As shown in Eq. (4), the amount of  $\cdot\text{OH}$  radicals produced with the FP is affected with solution pH and can be generated effectively in acidic conditions. The low  $\cdot\text{OH}$  radicals under high solution pH presumably related to formation and precipitation of  $\text{Fe}(\text{OH})_3$  according to Eqs. (4)–(10) [22].

### 3.2. Effect of contact time

In this step, for investigation of the effect of contact time on FP and PFP efficiency, the model dye solution with initial DR80 concentration of 40 mg/L at solution pH of 2 was prepared and after  $\text{Fe}^{2+}$  and  $\text{H}_2\text{O}_2$  addition (20 mg/L), the residual DR80 concentration analyzed after desired contact time. Fig. 3 shows variation of DR80 removal efficiency with FP and PFP under direct contact time.

As shown in Fig. 3, in case of FP, the highest DR80 removal efficiency was obtained after 35 min contact time and was equal to 81.2%. In this time, the residual DR80 concentration was 6.9 mg/L. Also, with increasing contact time

from 1 to 20 min, the DR80 removal with PFP was increased from 80.1% to 99.8% and the residual DR80 concentration decreased from 7.9 to 0.1 mg/L.

In both processes, it is clear that increasing the removal efficiency was faster at early contact times and then linear and slow. The slowly and linear increase in the removal efficiency might be related to the chemical oxidation of DR80 by  $\cdot\text{OH}$  radicals. The high concentrations of  $\cdot\text{OH}$  radicals are produced in the early minutes and DR80 can specifically be decreased, the  $\cdot\text{OH}$  radicals have extremely high oxidizing ability, that breakup organic compounds in a short contact time [23]. The reported optimum contact time for FP and PFP is short and is in agreement with our study, achieving to high efficiency at short contact time is so important in PFP because the cost of using electric light sources is about 60% of the total cost, the shortest reaction time, the least process cost [22,24].

### 3.3. Effect of $\text{Fe}^{2+}$ concentration

Variation of DR80 removal by FP and PFP as a function of  $\text{Fe}^{2+}$  concentration was studied, and the obtained results are illustrated in Fig. 4.

According to Fig. 4, in case of FP, the increasing  $\text{Fe}^{2+}$  concentration from 5 to 35 mg/L led to DR80 removal efficiency

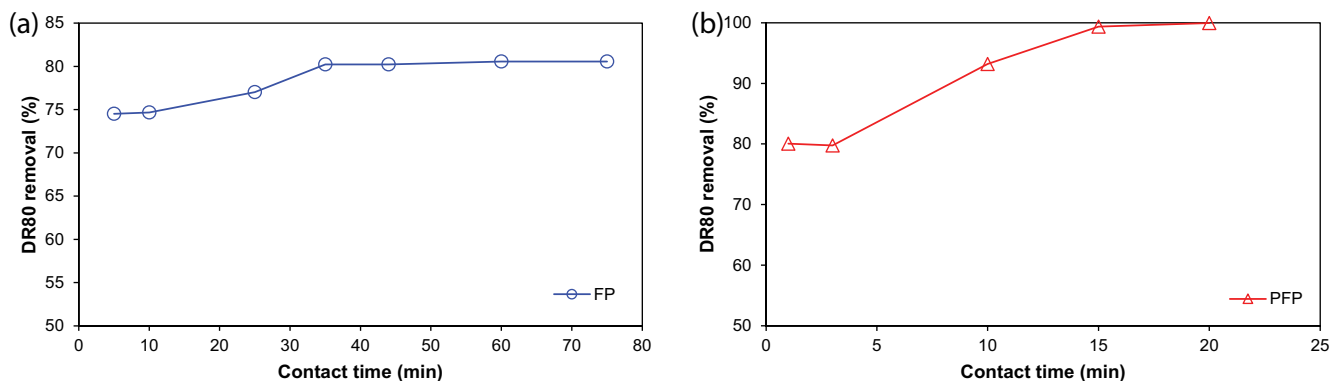


Fig. 3. Effect of contact time on DR80 removal by (a) FP and (b) PFP (initial DR80 concentration: 40 mg/L, solution pH: 2,  $\text{Fe}^{2+}$  concentration, 20 mg/L, and  $\text{H}_2\text{O}_2$  concentration: 20 mg/L).

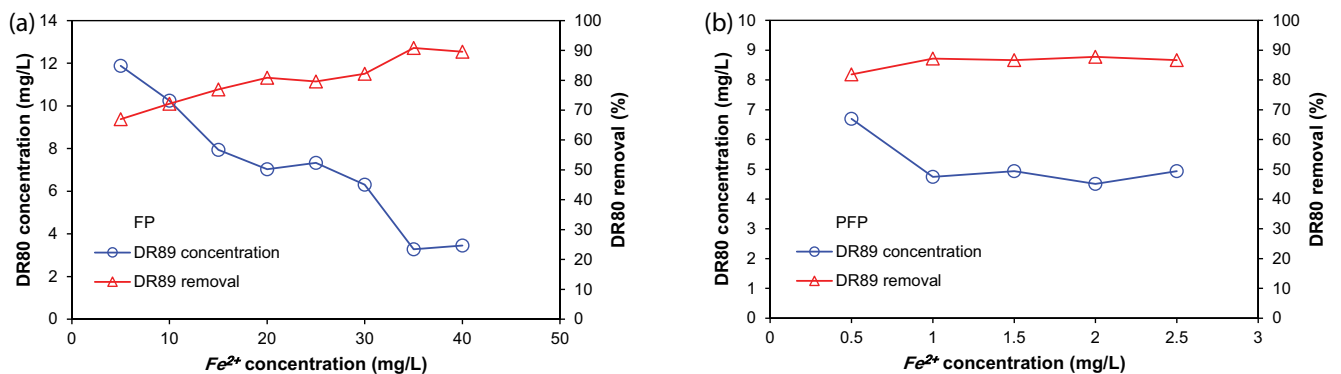


Fig. 4. DR80 removal by (a) FP and (b) PFP as a function of  $\text{Fe}^{2+}$  concentration (initial DR80 concentration: 40 mg/L, solution pH: 2,  $\text{H}_2\text{O}_2$  dose: 20 mg/L, contact time for FP: 35 min, and contact time for PFP: 20 min).

enhancing from 66.9% to 90.8%. But, by using Fe<sup>2+</sup> concentration higher than 35 mg/L, the DR80 removal efficiency was reduced to 89.5%. Also, Fig. 4 showed that with increasing Fe<sup>2+</sup> concentration from 0.5 to 2 mg/L, the removal efficiency of DR80 by PFP increased, and then, the DR80 removal remained almost constant with increasing Fe<sup>2+</sup> concentration. At Fe<sup>2+</sup> concentration of 2 mg/L, the residual DR80 concentration was 4.5 mg/L, indicating the highest removal efficiency of 87.8%.

One of the important parameters in FP and PFP is the concentration of Fe<sup>2+</sup> ions. The H<sub>2</sub>O<sub>2</sub> cannot oxidize some organic molecules in absences of Fe<sup>2+</sup> ion and with increasing Fe<sup>2+</sup> ion, the •OH radicals production increases and oxidation efficiency enhances [23]. As shown in Fig. 4, the removal efficiency of DR80 with FP and PFP was increased with increasing Fe<sup>2+</sup> concentration and is due to the higher production of •OH radicals [21]. Also, the result of experiments showed that the highest removal efficiency of DR80 by FP and PFP were accrued to 35 and 2 mg/L of Fe<sup>2+</sup> ions, respectively. Application of concentrations of Fe<sup>2+</sup> leads to the perhydroxyl radicals (HO<sub>2</sub>•) production while at lower concentrations of Fe<sup>2+</sup>, the •OH radicals generates that is more reactive than HO<sub>2</sub>• radicals. In addition, with increasing the Fe<sup>2+</sup> ions above these values, removal efficiency did not increase because of the tendency of the •OH radicals to react with Fe<sup>2+</sup> and H<sub>2</sub>O<sub>2</sub> in the oxidation–reduction reaction. With increasing the amount of Fe<sup>2+</sup> ion in solution, this substance transformed the •OH radicals into the hydroxide ions according to Eqs. (15) and (16) [23,25].



In addition, in case of PFP, higher Fe<sup>2+</sup> concentration made the solution brown and caused turbidity in solution. As a result, the created turbidity caused removal efficiency decreases by prevention of the UV radiation absorption that needed for photolysis [23]. The results obtained in the study

are in line with conducted study by Torrades and García-Montaña [25] in the removal of dye from the real wastewater, as well as the study conducted by Katsumata et al. [26] on the removal of reactive yellow 86 dye confirmed our results in this regard.

### 3.4. Effect of H<sub>2</sub>O<sub>2</sub> dose

In order to examine effect of H<sub>2</sub>O<sub>2</sub> dose on removal efficiency of FP and PFP, experiments were performed by application of various dose of H<sub>2</sub>O<sub>2</sub> in FP and PFP. The obtained results on effect of H<sub>2</sub>O<sub>2</sub> dose on dr89 removal efficiency by FP and PFP removal are illustrated in Fig. 5.

The results of DR80 removal by FP indicating with increasing H<sub>2</sub>O<sub>2</sub> dose from 20 to 80 mg/L, the DR80 removal efficiency increased from 79.1% to 92.2%. But application of H<sub>2</sub>O<sub>2</sub> dose higher than 80 mg/L, the removal efficiency of DR80 not significantly improved. Moreover, results of PFP demonstrated that when dose of H<sub>2</sub>O<sub>2</sub> is 2.5 mg/L, the DR80 removal efficiency was 78.8% and enhanced to 95.5% by increasing H<sub>2</sub>O<sub>2</sub> dose to 15 mg/L. As shown in Fig. 5, the increasing removal efficiency with increasing H<sub>2</sub>O<sub>2</sub> dose is related to the production of high amount of •OH radicals in presence of higher concentration of H<sub>2</sub>O<sub>2</sub> [4].

When H<sub>2</sub>O<sub>2</sub> was used higher than optimum dose, the excess amounts of H<sub>2</sub>O<sub>2</sub> react with •OH radicals to produce weaker radicals that are less active than •OH radicals as shown in Eq. (17) [14].



Furthermore, this behavior may be due to the spontaneous decomposition of H<sub>2</sub>O<sub>2</sub> into H<sub>2</sub>O and O, which reduced removal efficiency [27].

Al-Kahtani and Abou Taleb [28] studied Maxilon dye removal by PFP and found that with increasing H<sub>2</sub>O<sub>2</sub> dose, the dye removal efficiency decreased. Moreover, Sohrabi et al. [18] investigated removal efficiency of carmoisine edible dye by FP and PFP and reported that with increasing H<sub>2</sub>O<sub>2</sub> dose, the removal efficiency enhanced.

Table 1  
Experimental conditions employed in FP and PFP for DR80 removal

Process type	Studied parameter	Experimental conditions				
		Solution pH	Contact time (min)	Fe <sup>2+</sup> concentration (mg/L)	H <sub>2</sub> O <sub>2</sub> dose (mg/L)	DR80 concentration (mg/L)
FP	Solution pH	2–9	60	20	20	40
	Contact time	2	5–75	20	20	40
	Fe <sup>2+</sup> concentration	2	35	5–40	20	40
	H <sub>2</sub> O <sub>2</sub> dose	2	35	35	20–105	40
	DR80 concentration	2	35	35	80	20–90
PFP	Solution pH	2–9	60	20	20	40
	Contact time	2	1–20	20	20	40
	Fe <sup>2+</sup> concentration	2	20	0.075–2.5	20	40
	H <sub>2</sub> O <sub>2</sub> dose	2	20	2	2.5–15	40
	DR80 concentration	2	20	2	15	20–90

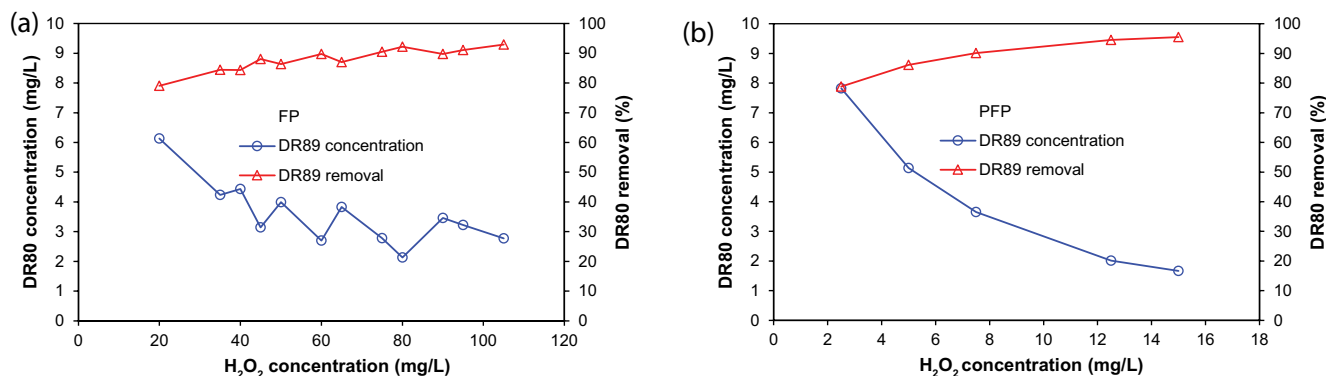


Fig. 5. Variation of DR80 removal by FP and PFP in respect of H<sub>2</sub>O<sub>2</sub> dose (initial DR80 concentration: 40 mg/L, solution pH: 2, contact time for EP: 35 min, Fe<sup>2+</sup> concentration in FP: 35 mg/L, and contact time for PEP: 20 min, Fe<sup>2+</sup> concentration in PFP: 2 mg/L).

### 3.5. Effect of initial DR80 concentration

In this step, experiments were conducted with various initial DR80 concentration under optimum conditions. Fig. 6 gives variation of DR80 removal efficiency by FP and PFP under optimum conditions at different initial DR80 concentration.

As seen in Fig. 6, the highest removal efficiency of DR80 by FP and PFP were documented at lowest DR80 concentration (20 mg/L) and were equal to 95.5% and 99.9%, respectively. The increasing initial DR80 concentration leading to reduction in removal efficiency. The increase of initial DR80 concentration from 20 to 90 mg/L was coincide decolorization reduction from 95% to 79% by FP and from 99.9% to 78.8% in PFP. Indeed, two mechanisms were proposed for decreasing removal efficiency at a high initial concentration including (i) as the catalyst and H<sub>2</sub>O<sub>2</sub> dose are constant, the performance of the active radicals will remain constant, so increasing in dye concentration, resulted in decreasing of removal efficiency, and (ii) at higher dye concentrations, the higher UV light absorption lead to inhibition of the H<sub>2</sub>O<sub>2</sub> photolysis and resulted in reduces the production of active elements [29]. In other words, when the dye concentration is increased, most of the UV radiation is absorbed with the dye molecules instead of H<sub>2</sub>O<sub>2</sub> and consequently, the production of •OH radicals decreases. As a result, removal of dye is reduced [18]. In this regard, similar results were observed by Modirshahla et al. [20] on removal of acid yellow 23 dye. Moreover, Mansoorian et al. [23] showed that with increasing dye concentration from 10 to 500 mg/L, the PFP efficiency decreased.

The partial oxidation of DR80 leading to formation of benzene and naphthalene rings and further oxidation (complete oxidation) resulted in CO<sub>2</sub> and H<sub>2</sub>O production [8]. The –N=N– bond of the DR80 dye is the most active site for oxidation attack [30] and Byberg et al. [31] demonstrates that the nitrogen atom of amino groups will first be transformed into NH<sub>4</sub><sup>+</sup> and later oxidized toward nitrates and finally evolved toward N<sub>2</sub>.

### 3.6. Empirical modeling

Despite several studies on application of AOPs for treatment of dye wastewater, the predication of treatment

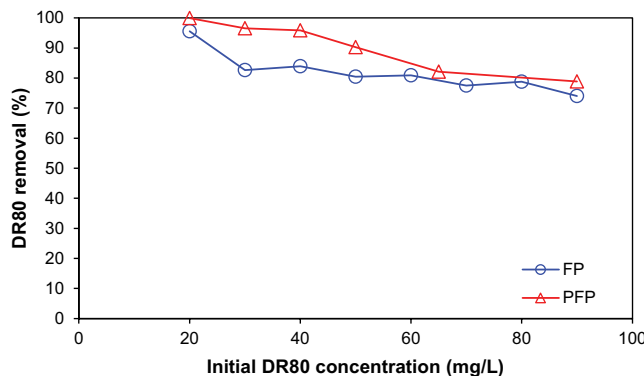


Fig. 6. Effect of initial DR80 concentration on removal efficiency of FP (H<sub>2</sub>O<sub>2</sub> concentration: 80 mg/L, solution pH: 2, contact time: 35 min, and Fe<sup>2+</sup> concentration: 35 mg/L) and PFP (H<sub>2</sub>O<sub>2</sub> concentration: 15 mg/L, solution pH: 2, contact time: 20 min, and Fe<sup>2+</sup> concentration: 2 mg/L).

efficiency of AOPs for dye wastewater may be difficult because of a lack of mathematical models. In this study, the results of five sets of experiments describing the effects of major operating variables including solution pH, contact time, Fe<sup>2+</sup> concentration, H<sub>2</sub>O<sub>2</sub> dose, and initial DR80 concentration on DR80 removal by FP and PFP were used for the development of empirical models according to previous study [32]. The DR80 removal as functions of operating variables presented in the previous sections were correlated with an empirical equation as Eq. (18).

$$E_r = 1 - \frac{S}{S_0} = a(\text{pH})^b (T)^c (\text{Fe})^d (\text{H}_2\text{O}_2)^e (S_0)^f \quad (18)$$

where  $E_r$  is DR80 removal rate,  $S_0$  is influent dye concentration, pH is solution pH,  $T$  is contact time, Fe is concentration of Fe<sup>2+</sup>, H<sub>2</sub>O<sub>2</sub> is applied hydrogen peroxide concentration and  $a$ ,  $b$ ,  $c$ ,  $d$ ,  $e$ , and  $f$  are constant values. The linearized forms of Eq. (18) may be written as Eq. (19).

$$\ln E_r = \ln a + b \ln(\text{pH}) + c \ln(T) + d \ln(\text{Fe}) + e \ln(\text{H}_2\text{O}_2) + f \ln(S_0) \quad (19)$$

The *b*, *c*, *d*, *e*, and *f* values were determined from the slope of the best fit line of  $\ln E_r$  vs.  $\ln$  of studied variables as presented in Table 2.

For example, to determine the constant *b* of Eq. (19), the experimental data obtained at varying solution pH (2–9) as shown Fig. 2, were plotted in the form of  $\ln E_r$  vs.  $\ln pH$ . So, from the slope of the best fit line, the *b* constant was found to be  $-0.37$  for FP and  $-0.28$  for PFP. The DR80 removal rate by FP and PFP were modeled by the polynomial equation as Eqs. (20) and (21), respectively.

$$E_r = 0.68(\text{pH})^{-0.37} (T)^{0.04} (\text{Fe})^{0.14} (\text{H}_2\text{O}_2)^{0.09} (S_0)^{-0.13} \quad (20)$$

$$E_r = 0.99(\text{pH})^{-0.28} (T)^{0.13} (\text{Fe})^{0.04} (\text{H}_2\text{O}_2)^{0.11} (S_0)^{-0.17} \quad (21)$$

As seen in Fig. 7, the plotting of experimental and predicted removal rate of DR80 by FP and PFP indicates good agreement between experimental and predicted data and also the value of  $R^2$  for empirical model was found to be 0.81 and 0.72, respectively.

Table 2  
Fit line of  $\ln E_r$  vs.  $\ln$  of studied variables

Plot	Process type	Linear equation	$R^2$
$\ln E_r$ vs. $\ln pH$	EF	$y = -0.37x + 4.74$	0.69
	PFP	$y = -0.28x + 4.86$	0.84
$\ln E_r$ vs. $\ln T$	EF	$y = 0.04x + 4.25$	0.91
	PFP	$y = 0.13x + 4.24$	0.99
$\ln E_r$ vs. $\ln Fe$	EF	$y = 0.14x + 3.9641$	0.92
	PFP	$y = 0.04x + 4.45$	0.67
$\ln E_r$ vs. $\ln H_2O_2$	EF	$y = 0.09x + 4.11$	0.90
	PFP	$y = 0.11x + 4.28$	0.99
$\ln E_r$ vs. $\ln S_0$	EF	$y = -0.13x + 4.93$	0.85
	PFP	$y = -0.17x + 5.14$	0.91

3.7. Sensitivity analysis

In present work, to determine effect of input parameters (assumptions) on the target forecast, the Monte Carlo

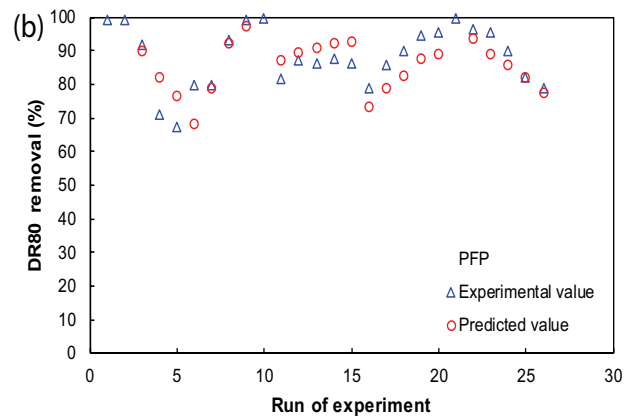
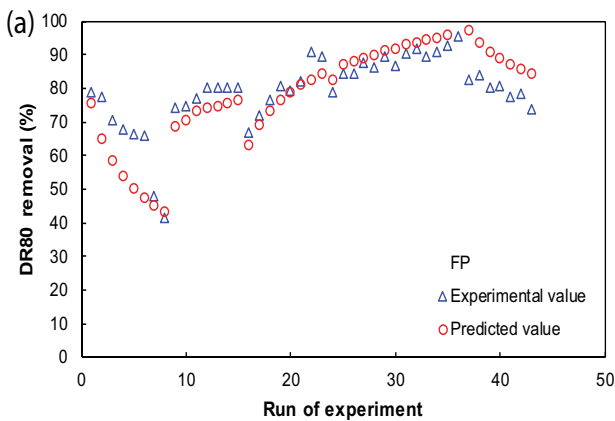


Fig. 7. Experimental value vs. predicted data on DR80 by FP and PFP.

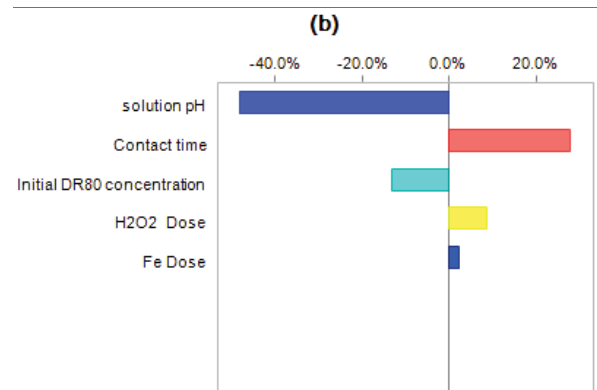
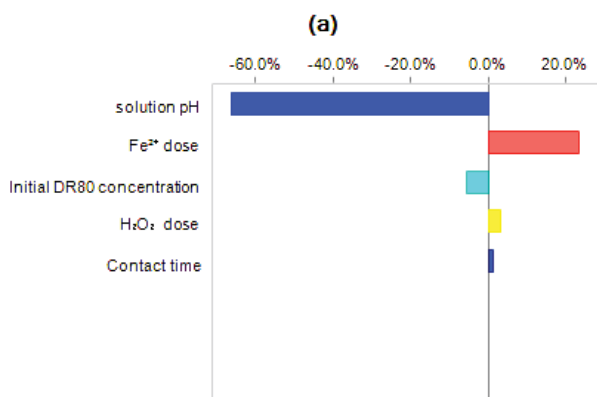


Fig. 8. Sensitivity chart for DR80 removal using (a) FP and (b) PFP.

Table 3  
Economic data for FP and PFP methodologies

Process	Sub-cost	Value
EP	Electrical power supplied for mixer (1,000 kW) and reactor volume (1 L)	–
	Required energy of UV lamp	1,000 W/1 L = 1,000 kW/m <sup>3</sup>
	Power consumption of mixer = required energy × treatment time	1,000 kW/m <sup>3</sup> × 0.6 h = 600 kWh/m <sup>3</sup>
	Cost of H <sub>2</sub> O <sub>2</sub> (70 \$/L) and optimum dose of H <sub>2</sub> O <sub>2</sub> : 80 mg/L or 0.08 L/m <sup>3</sup>	0.08 L/m <sup>3</sup> × 70 \$/L = 5.6 \$/m <sup>3</sup>
	Cost of Fe <sup>2+</sup> (68.4 \$/kg) and optimum dose of Fe <sup>2+</sup> : 35 mg/L or 35 g/m <sup>3</sup>	35 g/m <sup>3</sup> × 68.4 \$/kg = 2.39 \$/m <sup>3</sup>
	Total cost = cost of electrical energy (for industrial sector: 0.03 \$/kWh) + cost of chemicals	(600 × 0.03) + (2.39 + 5.6) = 25.99 \$/m <sup>3</sup>
PFP	Electrical power supplied for UV lamp (150 W) and reactor volume (1 L)	–
	Required energy of UV lamp	150 W/1 L = 150 kW/m <sup>3</sup>
	Power consumption of UV lamp = required energy × treatment time	150 kW/m <sup>3</sup> × 0.3 h = 45 kW/m <sup>3</sup>
	Power consumption of mixer	300 kWh/m <sup>3</sup>
	Cost of H <sub>2</sub> O <sub>2</sub> (70 \$/L) and optimum dose of H <sub>2</sub> O <sub>2</sub> : 15 mg/L or 0.015 L/m <sup>3</sup>	0.015 L/m <sup>3</sup> × 70 \$/L = 1.05 \$/m <sup>3</sup>
	Cost of Fe <sup>2+</sup> (68.4 \$/kg) and optimum dose of Fe <sup>2+</sup> : 2 mg/L or 2 g/m <sup>3</sup>	2 g L/m <sup>3</sup> × 68.4 \$/kg = 0.14 \$/m <sup>3</sup>
	Total cost = cost of electrical energy (for industrial sector: 0.03 \$/kWh) + cost of chemicals	(345 × 0.03) + (0.14 + 1.05) = 11.54 \$/m <sup>3</sup>

simulator using CRYSTAL BALL (11.1.2.4) software was run for 50,000 iterations. The solution pH, contact time, Fe<sup>2+</sup> concentration, H<sub>2</sub>O<sub>2</sub> dose, and initial DR80 concentration was defined as a assumptions with uniform distribution and the removal rate of DR80 ( $E_r$ ) was a target (output). The result of Monte Carlo simulation is shown in Fig. 8.

The positive value indicating the increasing effect of input parameters on target and negative coefficients revealed the opposite situation [33]. From Fig. 8, the solution pH has the greatest coefficient value of correlation and implying the strongest effect on DR80 removal rate. Based on magnitude impact of input parameters on DR80 removal rate, the assumptions rank for both FP and PFP was summarized in descending order as shown below:

For FP:

Solution pH > Fe<sup>2+</sup> concentration > initial DR80 concentration > H<sub>2</sub>O<sub>2</sub> dose > contact time

For PFP:

Solution pH > contact time > initial DR80 concentration > H<sub>2</sub>O<sub>2</sub> dose > Fe<sup>2+</sup> concentration

### 3.8. Cost evaluation for FP and PFP

The proposed methods by Korpe et al. [34] was used to conduction cost evaluation of different treatment process. To evaluation of cost of FP and PFP, the reactor with 1 m<sup>3</sup> capacity has been considered as summarized in Table 3.

As summarized in Table 3, the total cost of treatment by the FP and PFP were calculated to be 25.99 and 11.54 \$/m<sup>3</sup>, respectively. The significant difference between costs of both processes is due to the electrical energy of mixer for high contact time.

## 4. Conclusion

In present study, DR80 removal efficiency by FP and PFP were studied and effect of primary parameters on FP and PFP viz solution pH, contact time, Fe<sup>2+</sup> concentration, H<sub>2</sub>O<sub>2</sub> dose,

and initial DR80 concentration were systematically investigated. In addition, to predict DR80 removal efficiency during experiments, an empirical model was employed. Based on the conducted experiments, the following conclusions can be drawn.

- In FP and PFP, the DR80 removal efficiency was higher in acidic pH than alkaline pH.
- With increasing contact time, H<sub>2</sub>O<sub>2</sub> dose and Fe<sup>2+</sup> concentration, the DR80 removal efficiency increased.
- In FP with applying 20 mg/L of initial DR80 concentration, the highest removal efficiency was 95% and obtained at solution pH: 2, H<sub>2</sub>O<sub>2</sub> dose: 80 mg/L, Fe<sup>2+</sup> concentration: 35 mg/L, and 35 min contact time.
- When PFP was used, under optimum conditions (solution pH: 2, H<sub>2</sub>O<sub>2</sub> dose: 15 mg/L, Fe<sup>2+</sup> concentration: 2 mg/L, and 20 min contact time), the removal efficiency was 99.5% for 20 mg/L of DR80 concentration.
- The empirical model yielded a R<sup>2</sup> of 0.81 and 0.72 for FP and PFP, respectively, and relatively good describe DR80 removal efficiency under different conditions.
- Sensitivity analysis demonstrating solution pH has a strongest effect on DR80 removal rate in both processes.

## Acknowledgments

This work was financially supported by Student Research Committee, Isfahan University of Medical Sciences, Isfahan, Iran, under Project No. 194209. The authors express their thanks for this support.

## References

- [1] F. Gomri, M. Boutahala, H. Zaghoulane-Boudiaf, S.A. Korili, A. Gil, Removal of acid blue 80 from aqueous solutions by adsorption on chemical modified bentonites, *Desal. Water Treat.*, 57 (2016) 26240–26249.
- [2] M. Kamranifar, M. Khodadadi, V. Samiei, B. Dehdashti, M. Noori Sepehr, L. Rafati, N. Nasseh, Comparison the removal

- of reactive red 195 dye using powder and ash of barberry stem as a low cost adsorbent from aqueous solutions: isotherm and kinetic study, *J. Mol. Liq.*, 255 (2018) 572–577.
- [3] A. Dalvand, R. Nabizadeh, M. Reza Ganjali, M. Khoobi, S. Nazmara, A. Hossein Mahvi, Modeling of Reactive Blue 19 azo dye removal from colored textile wastewater using L-arginine-functionalized  $\text{Fe}_3\text{O}_4$  nanoparticles: optimization, reusability, kinetic and equilibrium studies, *J. Magn. Magn. Mater.*, 404 (2016) 179–189.
- [4] M.S. Lucas, J.A. Peres, Decolorization of the azo dye Reactive Black 5 by Fenton and photo-Fenton oxidation, *Dyes Pigm.*, 71 (2006) 236–244.
- [5] M. Kamranifar, A. Naghizadeh, Montmorillonite nanoparticles in removal of textile dyes from aqueous solutions: study of kinetics and thermodynamics, *Iran. J. Chem. Chem. Eng.*, 36 (2017) 127–137.
- [6] A. Naghizadeh, M. Kamranifar, A.R. Yari, M.J. Mohammadi, Equilibrium and kinetics study of reactive dyes removal from aqueous solutions by bentonite nanoparticles, *Desal. Water Treat.*, 97 (2017) 329–337.
- [7] J. de Jesus da Silveira Neta, G. Costa Moreira, C.J. da Silva, C. Reis, E.L. Reis, Use of polyurethane foams for the removal of the Direct Red 80 and Reactive Blue 21 dyes in aqueous medium, *Desalination*, 281 (2011) 55–60.
- [8] N.M. Mahmoodi, M. Arami, N.Y. Limaee, N.S. Tabrizi, Decolorization and aromatic ring degradation kinetics of Direct Red 80 by UV oxidation in the presence of hydrogen peroxide utilizing  $\text{TiO}_2$  as a photocatalyst, *Chem. Eng. J.*, 112 (2005) 191–196.
- [9] S. Abo-Farha, Comparative study of oxidation of some azo dyes by different advanced oxidation processes: Fenton, Fenton-like, photo-Fenton and photo-Fenton-like, *J. Am. Sci.*, 6 (2010) 128–142.
- [10] F. Al-Momani, E. Touraud, J. Degorce-Dumas, J. Roussy, O. Thomas, Biodegradability enhancement of textile dyes and textile wastewater by VUV photolysis, *J. Photochem. Photobiol., A*, 153 (2002) 191–197.
- [11] Y. Yosofi, S.A. Mousavi, Sono-photo-Fenton degradation of Reactive Black 5 from aqueous solutions: performance and kinetics, *Desal. Water Treat.*, 174 (2020) 354–360.
- [12] H.-F. Miao, M. Cao, D.-Y. Xu, H.-Y. Ren, M.-X. Zhao, Z.-X. Huang, W.-Q. Ruan, Degradation of phenazone in aqueous solution with ozone: influencing factors and degradation pathways, *Chemosphere*, 119 (2015) 326–333.
- [13] H. Lachheb, E. Puzenat, A. Houas, M. Ksibi, E. Elaloui, C. Guillard, J.-M. Herrmann, Photocatalytic degradation of various types of dyes (Alizarin S, Crocein Orange G, Methyl Red, Congo Red, Methylene Blue) in water by UV-irradiated titania, *Appl. Catal., B*, 39 (2002) 75–90.
- [14] M.A. Oturan, J.-J. Aaron, Advanced oxidation processes in water/wastewater treatment: principles and applications. A review, *Crit. Rev. Environ. Sci. Technol.*, 44 (2014) 2577–2641.
- [15] M. Malakootian, Performance evaluation of photo-Fenton process in removal of Acid Green 20 dye from wastewater of textile industries, *J. Rafsanjan Univ. Med. Sci.*, 14 (2016) 827–840.
- [16] V. Romero, S. Acevedo, P. Marco, J. Giménez, S. Esplugas, Enhancement of Fenton and photo-Fenton processes at initial circumneutral pH for the degradation of the  $\beta$ -blocker metoprolol, *Water Res.*, 88 (2016) 449–457.
- [17] J.-B. Tarkwa, N. Oturan, E. Acayanka, S. Laminsi, M.A. Oturan, Photo-Fenton oxidation of Orange G azo dye: process optimization and mineralization mechanism, *Environ. Chem. Lett.*, 17 (2019) 473–479.
- [18] M.R. Sohrabi, A. Khavaran, S. Shariati, S. Shariati, Removal of Carmoisine edible dye by Fenton and photo Fenton processes using Taguchi orthogonal array design, *Arabian J. Chem.*, 10 (2017) S3523–S3531.
- [19] A. Mousavi, P. Mohammadi, M. Parastar, M. Qaezbadeh, F. Kamari, Efficiency of Fenton oxidation in rodamine B removal from synthetic solutions, *J. Water Wastewater*, 6 (2014) 122–129.
- [20] N. Modirshahla, M.A. Behnajady, F. Ghanbary, Decolorization and mineralization of C.I. Acid Yellow 23 by Fenton and photo-Fenton processes, *Dyes Pigm.*, 73 (2007) 305–310.
- [21] M. Muruganandham, M. Swaminathan, Decolourisation of Reactive Orange 4 by Fenton and photo-Fenton oxidation technology, *Dyes Pigm.*, 63 (2004) 315–321.
- [22] M. Neamtu, A. Yediler, I. Siminiceanu, A. Kettrup, Oxidation of commercial reactive azo dye aqueous solutions by the photo-Fenton and Fenton-like processes, *J. Photochem. Photobiol., A*, 161 (2003) 87–93.
- [23] H.J. Mansoorian, E. Bazrafshan, A. Yari, M. Alizadeh, Removal of azo dyes from aqueous solution using Fenton and modified Fenton processes, *Health Scope*, 3 (2019) 1–9.
- [24] E.E. Ebrahiem, M.N. Al-Maghrabi, A.R. Mobarki, Removal of organic pollutants from industrial wastewater by applying photo-Fenton oxidation technology, *Arabian J. Chem.*, 10 (2017) S1674–S1679.
- [25] F. Torrades, J. García-Montaño, Using central composite experimental design to optimize the degradation of real dye wastewater by Fenton and photo-Fenton reactions, *Dyes Pigm.*, 100 (2014) 184–189.
- [26] H. Katsumata, S. Koike, S. Kaneco, T. Suzuki, K. Ohta, Degradation of Reactive Yellow 86 with photo-Fenton process driven by solar light, *J. Environ. Sci.*, 22 (2010) 1455–1461.
- [27] S. Mirzaei, M. Farzadkia, A. Jonidi Jafari, A. Esrafil, Removal of paraquat from aqueous solution using Fenton and Fenton-like processes, *J. Mazandaran Univ. Med. Sci.*, 27 (2017) 151–166.
- [28] A.A. Al-Kahtani, M.F. Abou Taleb, Photocatalytic degradation of Maxilon C.I. basic dye using  $\text{CS/CoFe}_2\text{O}_4/\text{GONCs}$  as a heterogeneous photo-Fenton catalyst prepared by gamma irradiation, *J. Hazard. Mater.*, 309 (2016) 10–19.
- [29] B.-L. Fei, J.-K. Zhong, N.-P. Deng, J.-H. Wang, Q.-B. Liu, Y.-G. Li, X. Mei, A novel 3D heteropoly blue type photo-Fenton-like catalyst and its ability to remove dye pollution, *Chemosphere*, 197 (2018) 241–250.
- [30] Z. Sun, Y. Chen, Q. Ke, Y. Yang, J. Yuan, Photocatalytic degradation of a cationic azo dye by  $\text{TiO}_2/\text{bentonite}$  nanocomposite, *J. Photochem. Photobiol., A*, 149 (2002) 169–174.
- [31] R. Byberg, J. Cobb, L.D. Martin, R.W. Thompson, T.A. Camezano, O. Zahraa, M.N. Pons, Comparison of photocatalytic degradation of dyes in relation to their structure, *Environ. Sci. Pollut. Res.*, 20 (2013) 3570–3581.
- [32] M. Khajeh, M.M. Amin, E. Taheri, A. Fatehizadeh, G. McKay, Influence of co-existing cations and anions on removal of direct red 89 dye from synthetic wastewater by hydrodynamic cavitation process: an empirical modeling, *Ultrason. Sonochem.*, 67 (2020), doi: 10.1016/j.ultsonch.2020.105133.
- [33] ORACLE Help Center, Oracle® Crystal Ball User's Guide, 2020, pp. 1–11.
- [34] S. Korpe, B. Bethi, S.H. Sonawane, K.V. Jayakumar, Tannery wastewater treatment by cavitation combined with advanced oxidation process (AOP), *Ultrason. Sonochem.*, 59 (2019) 1–9.